



Research Article

Fluconazole Nanosuspension Enhances *In Vitro* Antifungal Activity against Resistant Strains of *Candida albicans*

Katayoun Morteza-Semnani¹, Majid Saeedi², Jafar Akbari², Marvam Moazeni^{3,4}, Houman Seraj⁵, Elham Daftarifard⁵, Mahgol Tajbakhsh², Seyyed Mohammad Hassan Hashemi², Amirhossein Babaei²

¹Department of Medicinal Chemistry, Faculty of Pharmacy, Mazandaran University of Medical Sciences, Sari, Iran.

²Department of Pharmaceutics, Faculty of Pharmacy, Mazandaran University of Medical Sciences, Sari, Iran.

³Department of Medical Mycology and Parasitology, Faculty of Medicine, Mazandaran University of Medical Sciences, Sari, Iran.

⁴Invasive Fungi Research Centre, Communicable Disease Institute, Mazandaran University of Medical Sciences, Sari, Iran.

⁵Student Research Committee Center, Mazandaran University of Medical Sciences, Sari, Iran.

Article Info

Article History:

Received: 20 December 2020

Accepted: 15 April 2021

ePublished: 25 April 2021

Keywords:

- Anti-fungal
- Fluconazole
- Nanoparticles
- Nanosuspension
- Zeta potential

Abstract

Background: Recently, nanoparticles were widely used in drug delivery. Fluconazole (FLZ) is a lipid-soluble antifungal, which is utilized in treating fungal infections. The current work aimed to investigate the characteristics and antifungal activity of FLZ nanosuspension.

Methods: FLZ nanosuspensions were prepared by ultrasonication (simple and containing polymer). Surfactants in various concentrations were dissolved in the deionized water, and the drug powder was dispersed in the surfactant solution by a high-speed homogenizer to achieve nanosuspension. The polymer was added to the selected formula. FLZ nanosuspension characteristics, including polydispersity, mean particle size, entrapment efficacy, and zeta potential, were assessed. The release profile via dialysis membrane, differential scanning calorimetry (DSC), Fourier transform infrared spectroscopy (ATR-FTIR), and Transmission electron microscopy (TEM) were performed for nanosuspension evaluation. Antifungal activity against resistant strains of *Candida albicans* was defined according to the CLSI document guideline. To analyze the results, one-way ANOVA was used, followed by Tukey test.

Results: The results showed that increased sonication time and hydrophilic-lipophilic balance (HLB) significantly affected particle size reduction. Moreover, modification in the formulation components had a significant effect on the drug release process, furthermore affecting the properties of the nanoparticles. ATR-FTIR showed no chemical interaction between FLZ and formulation components. Compare to FLZ, a significant reduction ($p < 0.05$) was detected in the MIC values of both FLZ-resistant and FLZ-susceptible strains of *C. albicans* against FLZ nanosuspension.

Conclusion: It can be concluded that the ratio and amount of surfactants, the HLB, and the sonication process have effects on the properties of the nanoparticle's characteristics, and selected nanoparticles show suitable antifungal effect against resistant strains of *C. albicans*.

Introduction

In recent years, the prevalence of invasive fungal infections has risen. *C. albicans* are common human opportunistic fungal pathogen causing diseases ranging from mucosal to systemic infections for a variety of immunocompromised patients. The main risk factors for fungal infections are immunosuppression and the deterioration of anatomical defenses such as the skin. In numerous contexts, including AIDS, hospitals and intensive care, transplantation, and oncology units, physicians meet at-risk patients. The patients with severe and persistent neutropenia (hematological malignancy patients) are at higher risk; hence, they probably receive prophylactic treatment. By

taking practical measures, the patient can be prevented from exposing to fungi (regular hand washing, air filtration, avoiding flowers and plants); moreover, systemic fungal infection can be prevented by administering antifungal agents. Since fungal infections have mainly no specific symptoms, it is important to recognize the symptoms and signs of the disease, while this diagnosis is difficult and requires empirical treatments.¹

There are some limitations to antifungal agents. Many antifungals, such as azole derivatives, have poor solubility, which presents pharmaceutical formulation challenges in achieving effective therapeutic dosage forms.^{2,3} However, by novel formulations, therapy will be improved while

*Corresponding Author: Seyyed Mohammad Hassan Hashemi, E-mail: smhhashemipharma@gmail.com

©2021 The Author(s). This is an open access article and applies the Creative Commons Attribution License (<http://creativecommons.org/licenses/by-nc/4.0/>), which permits unrestricted use, distribution, and reproduction in any medium, as long as the original authors and source are cited.

playing the main role in future antifungal approaches.¹ Fluconazole (FLZ) is a third-generation triazole antifungal drug with wide-spectrum activity versus superficial fungal and systemic infections.^{4,5} It prevents the formation of essential principles within the fungal membrane as ergosterol through inhibition of the fungal cytochrome P-450 enzyme.⁶ It was found that in fungal species, such inhibition action on cytochrome P-450 enzymes is higher compared to the mammalian enzyme improving the triazoles' safety profile.⁷ FLZ is provided as parenteral and oral dosage forms causing severe adverse effects such as diarrhea, vomiting, rash, and reduced RBCs. Moreover, hepatotoxicity occurs in patients getting triazoles.⁸ FLZ with a molecular weight of 306.3 Da has a slight solubility in water and has a pKa value of 1.76 (weak base).^{9,10} Poor solubility of FLZ has made it difficult to form an effective drug delivery system.^{5,11}

The dissolution rate of poorly water soluble-drugs regularly becomes a rate-restraining phase in their absorption from the GI tract.¹²⁻¹⁴ There are several solubilizing approaches for increasing the dissolution features and drug solubilities, such as using a surfactant, polymeric conjugates, solid dispersion, and water-soluble carriers. It was found that preparing drugs as nanosuspensions is a more technically simpler and cost-effective alternative, mainly for poorly soluble drugs. It yields a product that is more stable physically compared to liposome dispersions.¹⁵⁻¹⁷ By such a method, grounding the drug dispersed in water is performed by shear forces to mean-diameter particles in the nanometer range (100 to 1000 nm). The nanoparticles are dissolved more quickly by their fineness since they have higher dissolution pressure, increasing their saturation solubility. It may improve the drugs' bioavailability in comparison to the other microparticulate systems. When the drug particles have a lower *in vivo* dissolution rate, the drug nanosuspensions will possess the passive targeting benefits of colloidal drug vehicles.¹⁸ Several nano-vehicles such as solid lipid nanoparticles (SLN) and nanostructured lipid carriers (NLC) can improve the FLZ effect against resistant *Candida* strains.¹⁹⁻²¹ Thus, trying to establish novel pharmaceutical dosage types of FLZ is greatly specified to prevent these side effects and improved its antifungal effect.

This research aimed to develop FLZ nanosuspension formulations as oral drug delivery systems to improve the dissolution rate of FLZ. The preparation of FLZ nanosuspension by the ultrasonic method as an eco-friendly technique was proposed. The improved formulation was assessed for *in vitro* dissolution profile and examine the effectiveness of FLZ by using an *in vitro* mycotic (*C. albicans*) infection model.

Materials and Methods

Material

FLZ was achieved as a gift specimen from Arasto Pharmaceuticals Chemicals Inc. (Tehran, Iran). PEG 200, Tween 20, and Span 80 were obtained from Merck Co.

(Germany). Eudragit RS & Eudragit RL were supplied by the Degussa Co. (Germany). Deionized water was purified by the Milli-Q system (Millipore, Direct-Q).

Preparing non-polymeric nanosuspension formulation

In this experimental study, ultrasonication was utilized to prepare FLZ nanoparticles in both types. The method was carried based on previous study.²² Briefly, FLZ nanosuspensions were prepared as follows: a certain amount of FLZ with PEG 200 and a half amount of span 80 transferred to a beaker. This mixture was placed on a heater stirrer with a temperature of 70° C. For aqueous phase preparation, Tween 20, half amount of Span 80 and water, was weighed accurately and homogenized with a high-speed homogenizer. The aqueous phase was placed on a warm-bath to reach a temperature of 70° C. In the next step, the aqueous phase was inserted to the lipid phase on the stirrer to become uniform. The formulation was sonicated by a probe sonicator (Bandelin, Germany) to reduce particle size and then transferred to the ice bath.

Preparation of polymeric nanosuspension formulation

For preparing polymeric-nanosuspension of FLZ, a certain amount of FLZ and Eudragit were weighed (Table 1), transferred to a beaker, and 30 ml of absolute alcohol was added to them and heated in a warm bath to melt the Eudragit. A certain amount of Tween 20 and water was then weighed and made uniform by a stirrer for aqueous phase preparation. The polymer and drug mixture were inserted into the aqueous phase slowly and stirred for 24h. The formulation was sonicated by probe sonicator (Bandelin, Germany) and Sonication bath (Pars Nahand, Iran) and transferred to an ice bath ultimately to reduce particle size.

Recognition of physicochemical features

Utilizing a Zetasizer Nano ZS system (Malvern Instruments, Worcestershire, the UK), the zeta potential, average particle size, and the PDI of FLZ-nanosuspension were measured via dynamic light scattering (DLS) technique at the ambient temperature with an angle of 90°. Taking three separate specimens for each formulation, the tests were performed three times with no dilution at room temperature.^{23,24}

Attenuated total reflectance-Fourier transform infrared spectroscopy

Using Cary 630 FTIR spectrophotometer (Agilent Technologies Inc., CA, USA) with a diamond ATR (Attenuated Total Reflectance), the FLZ-excipient interactions were assessed. Then, ATR-Fourier transform infrared (ATR-FTIR) spectroscopy was used to examine FLZ, Eudragit RSPO, Tween 20, and chosen formulations. Based on the above process, to record the spectra, a lower quantity for every homogeneous sample was placed on the slit, then scanning the specimens was performed from 4000-650 cm⁻¹ with a resolution of 2 cm⁻¹.²⁵

Differential scanning calorimetry

The thermal performance of the FLZ-nanosuspension and the pure drug was assessed using Differential scanning calorimetry (DSC). Before the heating procedure, about 4 mg of the specimens were weighed within the hermetic crimped aluminum pan, preserved for 15 min at 30 °C. Heating the specimens was performed to 160 °C under a nitrogen atmosphere at a scanning rate of 10 °C/min. Using Pyris 6 (Perkin Elmer, the USA), the DSC traces were evaluated. The DSC was calibrated using indium (melting transition of 429.75 K) as the standard.

Transmission electron microscopy

Using a Transmission electron microscopy (TEM) microscope (Philips CM 120 kV, Amsterdam, the Netherlands), the FLZ-nanosuspension morphology was examined. Hence, FLZ-nanosuspension drops were put on carbon-covered copper grids. By preparing a 2 % (v/v) phosphotungstic acid solution, the nanoparticles were negatively stained for 30 s.²⁶ Ultimately, the solvent was let for drying at room temperature overnight while administering TEM visualization.²⁷

Drug release

The drugs' release profile in nanosuspension is a pivotal factor in determining its efficiency. By dispersing the formulation in dissolution media (Phosphate buffer, pH of 6.8), the media specimens were eliminated at given profile intervals for measuring the amount of the drug released via UV-spectroscopy. The paddle technique (Type II) stated in US Pharmacopoeia (USP XXVIII, 2005) was used to determine the formulations' release profile. Using the Erweka dissolution apparatus (DT620, Erweka, Germany), the drug release tests were conducted. For the release test, almost 900 ml of dissolution medium was made at 37.0 °C, and 100 rpm was determined as the rotation speed. The specimens (5 ml) were then eliminated from the dissolution media at different time intervals (5, 10, 15, 30, 45 minutes, 1.5, 2, 4, 6, 8, and 24h) and substituted with fresh medium (at the same temperature). UV technique was used to assay the quantity of FLZ in specimens at 260 nm.²⁸

Antifungal susceptibility testing

Strains and Antifungal agents

Ten isolates of *C. albicans*, including five FLZ susceptible and five FLZ resistant, were tested in the current work. The isolates were recognized previously to the species level through sequencing the internal transcribed spacer (ITS1-5.8s-ITS2). FLZ-resistant *C. albicans* strains were previously confirmed to have MIC \geq 8 μ g/ml according to the CLSI guidelines.²⁹ To achieve significant growth of fresh viable yeast cells, the strains were cultured on yeast extract peptone dextrose agar (YEPD), including 10 g/L yeast extract (Difco-BD, the USA), 20 g/L glucose (Merck, Darmstadt, Germany), 20 g/L peptones (Difco-BD, USA), and 20 g/L agar (Merck, Darmstadt, Germany) and incubated for 48h in 35 °C. MICs were determined as

the least concentration of the antifungal agent at which the tested fungal isolates did not demonstrate visible growth.

Antifungal susceptibility testing for *Candida species* isolates

The F7 and F11 agents were distributed in a 96 well microplate. The final concentration of both agents was ranged from 0.125 to 64 μ g/ml. The yeast inoculum was made using a sterile saline solution with 75-77% of transmission at 530 nm. Accordingly, the inoculum concentration ranges of 1–5 \times 10⁶ CFU/ml were achieved.³⁰ The two times test inoculums (1 \times 10³ to 5 \times 10³ CFU/ml) concentration was achieved through a 1:10 dilution after a 1:100 dilution of the stock suspension in RPMI medium. Incubation of the plates was performed at 35°C and was visually read after 24h. The least inhibitory concentration values were determined as the drug's concentration inhibiting the 50% growth of the strains compared to a drug-free control. A quality control (*C. parapsilosis* ATCC 22019) was also run for each isolate in a new MIC plate series.

Determination of minimum fungicidal concentration

The minimum fungicidal concentrations (MFC) is defined as the minimum concentration at which the growth of the yeast is completely inhibited. The MFCs were determined by adding 200 μ l of yeast suspension from each well, having a concentration equal to and upwards of the MIC on Sabouraud Dextrose Agar (HiMedia, Mumbai, India) plates. The plates were incubated at 35°C for 48h, and the appearance of growth was noted.

In vitro non-specific cytotoxicity

The human gingival fibroblast cells (HGF3-PI53) were obtained from the National Cell Bank of Iran (Pasteur Institute of Iran; Tehran, Iran) and were seeded (10⁵ cells/well) to grow in a 96-well plate and were incubated for 24h. Following the initial incubation cycle, cells were treated for one day with various FLZ concentrations. Then, 100 μ l of MTT (5mg/ml) was applied for 3h to the cells. Next, the MTT was discarded, and 100 μ l of DMSO was added to dissolve the formazan produced during the procedure for 1h. Cell survival was determined as the absorbance percentage compared to the control absorbance. Different concentrations (1000, 600, 300, 150, 100, and 50 μ M) With Six additional controls, they were evaluated three times (the cells in medium). Ultimately, the cells' viability was determined using the following equation.

Viability (%) = [OD560(sample)/OD560 (control)] \times 100
 OD 560 (sample): the optical density (sample) at 560 nm.
 OD560 (control): the optical density (control) at 560 nm.

Data analysis and statistics

As mentioned earlier, the data were written as the mean \pm SD. Then, SPSS 22.0 (IBM Co., USA) was used to analyze the data. Analysis of variance (ANOVA) and Tukey's post-hoc test was utilized for statistically analyzing the defined variables. The P-value < 0.05 was quoted as statistically significant.

Results and Discussion

Nanosuspension features

Since the nanocarrier' size is a crucial feature for nanoparticles, it has obtained specific attention. The hydrodynamic diameter of nanoparticles is represented in Table 1. Moreover, the PDI reveals the dispersion's quality (as a sign of the particle size distribution's width). Typically, the PDI value is within the range of 0 to 1, and the PDI values less than 0.7 indicate the pervasive distribution of particle sizes.³¹

FLZ nanosuspensions were prepared at varying polymer concentrations, HLB, and the time of the ultrasonication. The results revealed that ultrasonication time significantly affected reducing the particle size in F1 and F2 with similar formulation composition. In addition to a decrease in particle size in F1 ($P = 0.0002$), the PDI and zeta potential reduced by decreasing in time of sonication from 0.59 ± 0.02 to 0.36 ± 0.06 , and electrical charge changes from -14.70 ± 0.55 to -11.80 ± 0.75 mV in F1 and F2, respectively. These results confirmed the effects of the ultrasonication process's duration on the particle size of dispersed drugs. This event was associated with the incremented erosion effects on the crystal agglomerates and large crystals surface. Dengning Xia *et al.*³² study on preparing stable nitrendipine nanosuspensions utilizing the precipitation-ultrasonication technique for improvement of oral bioavailability and dissolution. In this study, the ultrasonication time length also affected the particle size. For the power input of 400W, the nanocrystals' particle size was decreased by incrementing the ultrasonication time to 15 min.

To define the effects of surfactants concentration on the characteristics of FLZ nanosuspensions F2 and F3 with the

same HLB and different amount of surfactants composition were evaluated. The results indicated that no significant difference exists in particle size in F2 and F3 ($P = 0.0616$). Evaluation of nanoparticles in F3, F4, and F5 revealed that particle size decreased from 295.13 ± 14.45 to 107.26 ± 3.13 nm ($p < 0.001$) by an increase in the HLB value. The higher HLB value is, the more hydrophilic properties of the surfactant system. The hydrophilic mixture of surfactants should reveal a higher probability of interaction with the hydrophilic FLZ particles, yielding a smaller particle size. With increasing HLB value 10.5 to 16.7 in F3, F4, and F5, zeta potential changed significantly from -14.66 ± 0.56 to 9.54 ± 2.02 mV ($p < 0.0001$), but there was not observed any change in PDI value in these formulations (0.42 ± 0.02 in F3 and 0.56 ± 0.29 in F5, $P = 0.459$). The particles were formed within two phases, including the nucleation procedure within the droplet, then the aggregation procedure to create the ultimate particle. The nucleation rate was determined as the number of nuclei generated per unit volume/unit time. The particle growth rate is measured through mass transfer within the droplets. Into the droplets, the growth and nucleation happen and control the ultimate particle size. There is a very fast physical reaction within the droplet; hence, the rate-determination stage will be the initial communication phase of the microdroplets with various droplets. The fast growth of nuclei is prevented by the existence of surfactant strictly. Thus, the particles' growth will occur at a similar rate, favouring the creation of particles with higher homogeneous size distribution. A suspension of small particles is a resultant, stabilized by the surfactant molecules prohibiting coalescence where the system would result in further agglomeration without it. The nuclei's size will be affected by the droplets'

Table 1. The examined FLZ nanosuspension components and their physicochemical characteristics.

Code	Formulation composition (g)						Formulation condition				Formulation characteristics		
	FLZ	Tween 20	PEG	Span 80	Eudragit RS	Eudragit RL	Water	HLB	Temp	Sonication time	Size (nm)	PDI	Zeta potential (mV)
Non-polymeric	F1	0.8	3	2.2	3		80	10.5	100	10	81.42±9.16	0.59±0.02	-14.70±0.55
	F2	0.8	3	2.2	3		80	10.5	100	2.5	350.40±23.60	0.36±0.06	-11.80±0.75
	F3	0.8	2	2.2	2		80	10.5	100	2.5	295.13±14.45	0.42±0.02	-14.66±0.56
	F4	0.8	3	2.2	1		80	13.6	100	2.5	138.13±20.06	0.36±0.13	-9.42±2.97
	F5	1	4				92.5	16.7			107.26±3.13	0.56±0.29	9.54±2.02
Polymeric	F6	1	4		2.5		92.5	16.7			142.13±2.09	0.26±0.01	17.96±4.21
	F7	1	3		2.5		92.5	16.7			115.10±9.73	0.22±0.02	18.80±1.01
	F8	1	2		3		92.5	16.7			125.50±5.86	0.23±0.01	18.46±4.02
	F9	1	2		2.5		92.5	16.7			108.53±11.93	0.20±0.01	19.96±0.76
	F10	1	2		2		92.5	16.7			124.02±33.04	0.28±0.08	18.66±1.55
	F11	1	2		1.5		92.5	16.7			99.94±17.30	0.31±0.08	19.33±0.73

size; however, the surrounding surfactant molecules will control the final particle size.³³ The microemulsion system-generated solid particle size may be obtained from a lesser nucleation rate or greater nuclei growth rate. The surface energy is further reduced by the surfactant with less HLB (span 80) value, thus, the nucleation rate is increased. The smaller particle size and more hydrophilic features are indicated by the higher surfactant HLB number. The more lipophilic surfactant in an o/w microemulsion system results in the higher droplet size increasing the mass transfer quantities into the droplets. Hence, a higher nucleus growth and increased final particle size are caused by the lower HLB value for surfactant.

Eudragit was used as a coating polymer for stabilizing FLZ-nanosuspension. The results revealed a decrease in particle size in F8 to F11 compared with polymer formulations (Table 1). The Zeta potential and PDI changed in Eudragit containing nanosuspensions significantly too. The increment in particle size could be ascribed to the disperse phase viscosity since the supplied energy as agitation could not overwhelm viscous forces created by the formulation's higher solid content.³⁴ Moreover, particle aggregation is promoted by the higher solid content by incrementing the collision probability between particles existing in the aqueous phase.³⁵ Therefore, bigger mean particle sizes are obtained by higher viscosity. Generally, the obtained particle size data represented more association with the polymer amount.

In this study, the type of polymer was altered from Eudragit RL (F5) to Eudragit RS (F6). The nanosuspension size changed from 107.26 ± 3.13 to 142.13 ± 2.09 nm significantly ($p < 0.05$) in these formulations, respectively. The zeta potential of nanoparticles changed from 9.54 ± 2.02 to 17.96 ± 4.21 mV in F5, F6 significantly ($p < 0.05$). The PDI value decreased from 0.56 ± 0.29 to 0.26 ± 0.01 in these nanosuspensions, respectively ($p < 0.05$). Matlhola *et al.*³⁶ studied tenofovir nanoparticles with Eudragit RSPO. They showed a small mean particle size gained by a lower polymer/drug ratio of 1:1 (50 mg of a polymer/50 mg of a drug). There is a right consistency between such results and the findings of the present work. Existing this drug, a positive zeta-potential is maintained by the particles suggesting that the active compound is mainly distributed into the polymer matrix, in addition to the absorbance over their surface. Moreover, it is indicated that acidic compounds, such as azole groups, interact with RL and RS polymers through electrostatic bindings between their 1,2,4 triazole as well as the quaternary ammonium groups of the polymer.

Differential scanning calorimetry analysis

Figure 1 provides the DSC analysis findings for formulations and FLZ. Regarding the DSC thermograms, it was found that an endothermic peak is exhibited by FLZ at 140°C relevant to the FLZ melting point. Moreover, based on the formulations' endothermic peaks at 140 °C, it is found that there is no endothermic peak for FLZ. Such

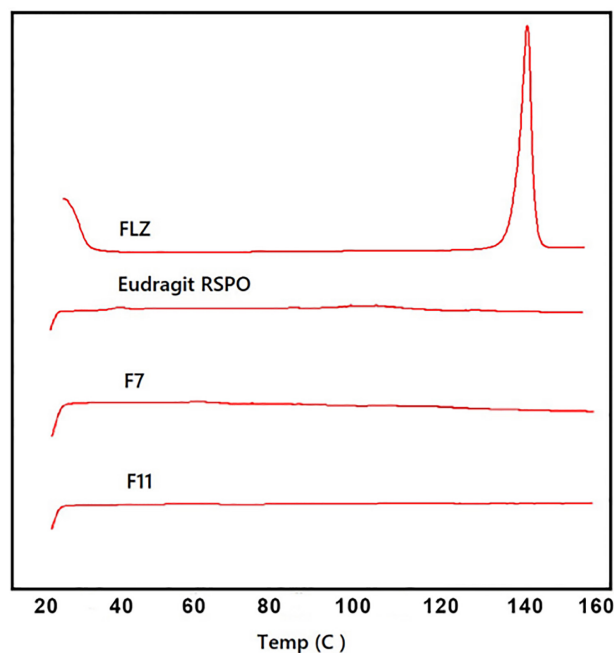


Figure 1. DSC curves of FLZ, Eudragit RSPO, F7 and F11.

observations could indicate the lower crystallinity of the drug in nanosuspension.

Attenuated total reflectance-Fourier transform infrared spectroscopic analysis

Using ATR-FTIR spectroscopy over nanosuspension formulations and pure raw materials, the possible interactions between components of the nanosuspension formulations were analyzed. The ATR-FTIR spectra were provided in Figure 2. The representative peaks of ATR-FTIR spectra of FLZ, Eudragit RSPO, and Tween 20 were summarized as follows: FLZ: $3400-3200$ cm^{-1} (O-H stretching), 3111 cm^{-1} (aromatic C-H stretching), $1618-1417$ cm^{-1} (aromatic C=C & C=N stretching), and 1271 cm^{-1} (C-F stretching). Eudragit RSPO: $3000-2850$ cm^{-1} (C-H stretching), 1722 cm^{-1} (C=O stretching), and 1141 cm^{-1} (C-O stretching). Tween 20: 3517 cm^{-1} (O-H stretching), 2921 cm^{-1} and 2858 cm^{-1} (aliphatic C-H stretching), and 1735 cm^{-1} (C=O stretching). There were no chemical interactions within the FLZ and other components of F7 and F11, based on the ATR-FTIR results.

Transmission electron microscopy analysis

The FLZ-nanosuspension's TEM images denoted that the nanoparticles have roughly uniform spherical shapes with mean sizes of 100-150 nm (Figure 3). There is no symbol of aggregation within the images; hence, the particle size was less than 150 nm.

Drug release

The drug bioavailability can be affected by the drug release from nanoparticles at controlled rates. The results were obtained by comparing the drug release from the dialysis membrane of the control with F4, F7, and F11, shown in Figure 4. The release of drug from nanosuspension (F4,

F11, and F7) were significantly higher than from control ($p < 0.05$). The percentage of drug release from F4, F11, F7, and control are 59.78 ± 4.65 , 28.51 ± 2.04 , 24.30 ± 0.83 , and 21.12 ± 0.50 , respectively. These results showed that the nanosuspension could increase dissolution rate, the bioavailability of the poorly soluble drug, and provide

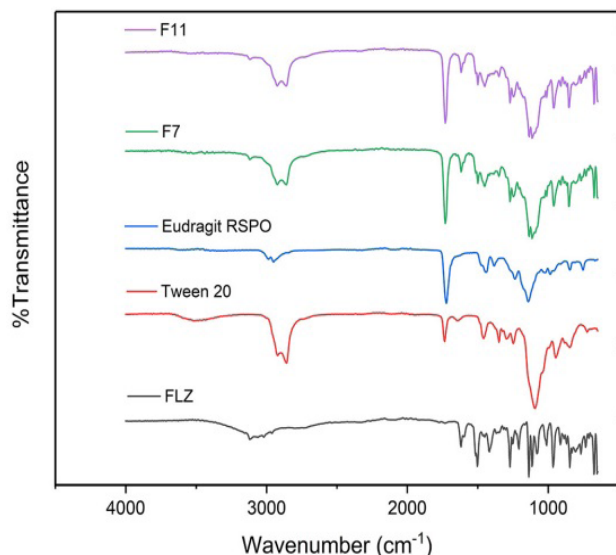


Figure 2. ATR-FTIR spectra of formulations F11, F7, Eudragit RSPO, Tween 20 and FLZ.

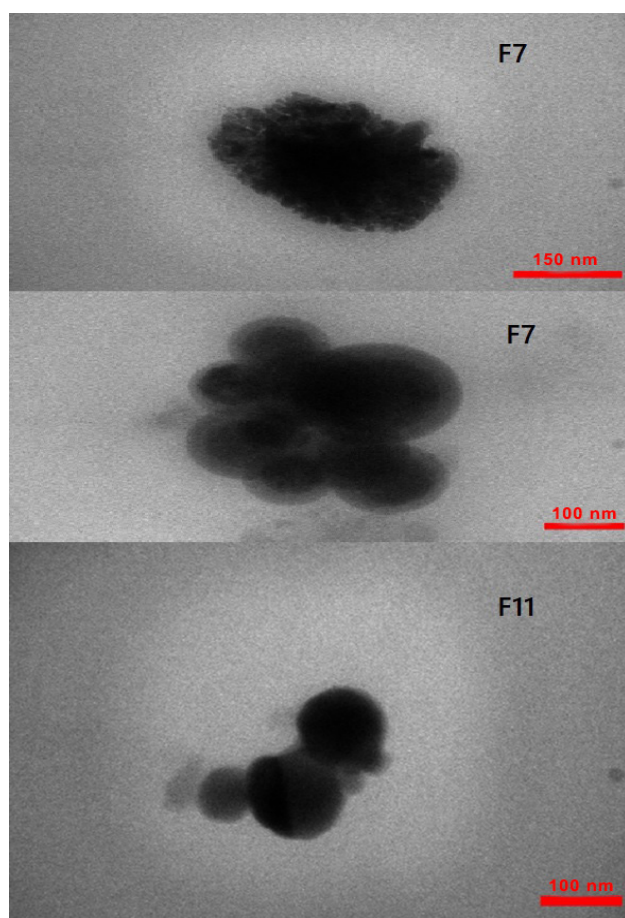


Figure 3. TEM of F7 and F11.

sustained drug release.

Nakrani *et al.*⁸ studied Itraconazole nanosuspension and showed the *in vitro* dissolution profile of the improved nanocarrier compared to the marketed formulation and pure drug (Canditral Capsule) utilizing 0.1 N Hydrochloric acid as a medium, which revealed a more significant drug release. Shid *et al.*³⁷ reported that simvastatin-loaded nano-suspension considerably enhanced *in vitro* dissolution rate; thus, it possibly improves quick start of therapeutic drug impact. Based on the *in vivo* study, bioavailability increases in nanosuspension formulation compared to the plain simvastatin drug.

Antifungal susceptibility testing

Table 2 represents the detailed findings for antifungal susceptibility profile (MICs and MFCs) of F7 and F11 against 10 *C. albicans* strains. The isolates resistant to FLZ revealed a considerable reduction in MIC values by utilizing FLZ nanosuspension as their MIC value within the sensitive range. Also, for FLZ-susceptible strains, the MIC values were significantly ($p < 0.05$) decreased compared to FLZ alone. No differences were observed in MIC90 values for all isolates as it was found to be 0.5 and 0.25 $\mu\text{g/ml}$ for FLZ-resistant and FLZ-susceptible isolates, respectively. Hence, the antifungal inhibitory effect of both formulations seems to be the same. It was interesting to note that when F7 and F11 formulations were employed, the MICs values were significantly reduced compared to FLZ on its own. MFCs of F7 and F11 spanned a wide range (2-16 $\mu\text{g/ml}$) since FLZ has mostly fungistatic action *in vivo*, even at therapeutic doses. However, it is suggested that the therapeutic dose could be decreased, which may decrease the risk of adverse drug impacts. Similar results were observed in FLZ nanoparticles as NLC and SLN. MIC values were reduced by solid lipid nanoparticles of FLZ for FLZ-susceptible strains of *C. albicans*, *C. glabrata*, and *C. parapsilosis* significantly ($p < 0.05$).¹⁹ In another study *C. albicans* isolates revealed further susceptibility to FLZ-loaded nanostructured lipid carriers compared

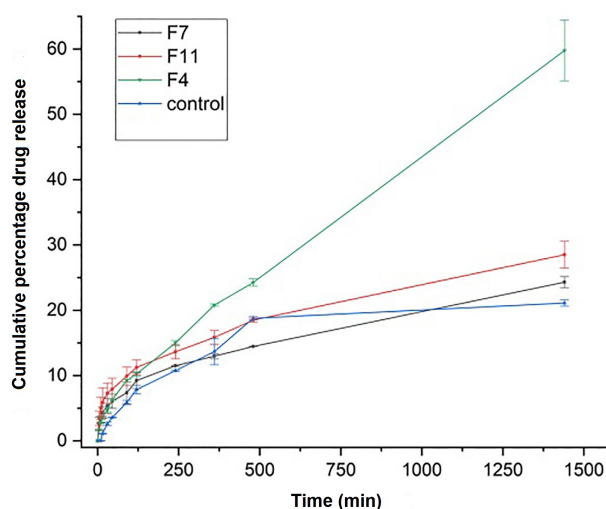


Figure 4. In vitro drug release control, F4, F7 and F11.

Table 2. Effect of new FLZ formulations *C. albicans* stains.

Isolates	MICs/ MFCs ($\mu\text{g/ml}$)												
	FLZ				F7				F11				
	MIC	MIC90	GM	MFC	MIC	MIC90	GM	MFC	MIC	MIC90	GM	MFC	
FLZ-resistant isolates	<i>C. albicans</i> MZ 24	>64			>64	0.25			8	0.25			8
	<i>C. albicans</i> MZ 25	>64			>64	0.5			16	0.5			16
	<i>C. albicans</i> MZ 27	>64	64	64	>64	0.5	0.5	0.3298	16	0.5	0.5	0.3789	16
	<i>C. albicans</i> MZ 28	>64			>64	0.25			8	0.5			16
	<i>C. albicans</i> MZ 29	>64			>64	0.25			8	0.25			8
FLZ-susceptible isolates	<i>C. albicans</i> MZ 2	0.25			4	0.0625			2	0.125			4
	<i>C. albicans</i> MZ 9	0.5			8	0.25			8	0.25			8
	<i>C. albicans</i> MZ 1	0.5	0.5	0.3789	8	0.25	0.25	0.1435	8	0.25	0.25	0.1894	8
	<i>C. albicans</i> MZ 3	0.25			8	0.0625			4	0.125			4
	<i>C. albicans</i> MZ 4	0.5			8	0.25			8	0.25			8

to simple drug dispersion. The MIC of FLZ decreased significantly in FLZ-NLCs in several *Candida* species.²⁰ In another study, the effect of SLN and NLC nanoparticles of FLZ were evaluated against resistant strains of *C. albicans*. A considerable reduction was found in MIC values by applying both novel formulations. Nevertheless, FLZ-NLC was more effective than FLZ-SLNs ($p < 0.05$).²¹

A possible clarification for the antifungal susceptibility findings is the mechanism in charge of the drug resistance identified in pathogenic fungi. Moreover, the drug resistance mechanisms can occur in three different modes, including reduced drug concentration occurring to drug efflux, a mutation in the genome sequence, and alteration in the drug target.^{38,39} The plasma membrane overexpression carries proteins pumping the azoles out of cells. This is a common mechanism of high-level azole resistance in fungi.⁴⁰ In this work, an effective nano-scaled safeguard is provided by FLZ nanosuspensions while protecting the drug from pumping out by transporter proteins. Furthermore, the drug enters the yeast cells more efficiently, more quickly, and more easily by the FLZ nanosuspensions hydrophobic surface.

MTT assay

Drug nanoparticles are well believed to cause toxic effects on body organs, and nanoparticles are more easily transfected into cells, increasing toxicity. Also, nanoparticles' surface charge may cause an increase in cell and protein reactivity. MTT analyses have also been used as an indicator of cell viability, proliferation, and cytotoxicity to assess metabolic activities.⁴¹ MTT was applied in the present study to evaluate the cell viability of FLZ nanosuspension. Different concentrations of free FLZ solution (as stated above), FLZ nanosuspension (F7 and F11), and blank nanosuspension were tested for this

purpose at 50-1000 μM . The cells were incubated for 24h during the cell viability test using the HGF PI53 normal fibroblast cell line obtained from the Pastor Institute (Tehran, Iran). In the presence of blank nanosuspension, FLZ, F7, and F11, the cell viability was not significantly decreased over 24h. ($p > 0.05$) (Figure 5). The authors were unable to find research on cytotoxicity caused by FLZ. *In vitro*, nevertheless, necrosis can be due to the cytotoxic effects caused by FLZ in rat hepatocytes *in vitro* as evaluated with the LDH assay.⁴² Correa *et al.*⁴³ examined the cytotoxic and genotoxic effects of FLZ on the African Green Monkey Kidney cell line (Vero). The Vero cell line was exposed to various FLZ concentrations *in vitro* and then assessed for various factors, such as cytotoxicity (MTT assay). MTT showed that cell viability decreased a little when exposed to

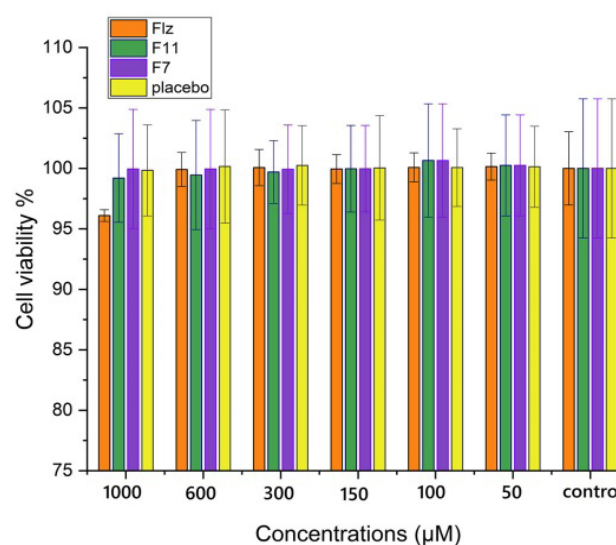


Figure 5. Cell viability of different concentrations of FLZ solution, F7, F11 and blank nanosuspension. Data are expressed as mean \pm SD.

FLZ in 1306 μ M (cell viability over than 85%).

Conclusion

It is found that nanocrystalline suspensions of weakly soluble drugs like FLZ are easily prepared and to lyophilized for prolonged storage while representing an encouraging novel drug formulation for oral drug delivery for treating fungal infections. Dissolution study indicated that higher drug release is provided by nanosuspension formulation in comparison to the pure one. Thus, a promising alternative is represented by nanosuspensions to existing delivery systems aimed to enhance the biopharmaceutical performance of drugs with lower water solubility.

Author Contributions

KMS: Conceptualization, visualisation. MS: Supervision, formal analysis. JA: Supervision, methodology. MM: Formal analysis. HS: Investigation. ED: Investigation. MT: Formal analysis. SMHH: Writing-original draft. AB: Writing-review and editing. All authors read and approved the manuscript.

Acknowledgments

This study was funded by a grant from the Mazandaran University of Medical Sciences Research Council, Sari, Iran.

Conflict of Interest

The authors claim that there is no conflict of interest.

References

- Maertens J, Vrebos M, Boogaerts M. Assessing risk factors for systemic fungal infections. *Eur J Cancer Care (Engl)*. 2001;10(1):56-62. doi:10.1046/j.1365-2354.2001.00241.x
- Yang W, Wiederhold NP, Williams III RO. Drug delivery strategies for improved azole antifungal action. *Expert Opin Drug Deliv*. 2008;5(11):1199-216. doi:10.1517/17425240802457188
- Vlaia L, Coneac G, Muş AM, Olariu I, Vlaia V, Anghel DE, et al. Topical biocompatible fluconazole-loaded microemulsions based on essential oils and sucrose esters: Formulation design based on pseudo-ternary phase diagrams and physicochemical characterization. *Processes*. 2021;9(1):144.
- Ruhnke M, Hartwig K, Kofla G. New options for treatment of candidaemia in critically ill patients. *Clin Microbiol Infect*. 2008;14:46-54. doi:10.1111/j.1469-0691.2008.01981.x
- Abdellatif AAH, El-Telbany DFA, Zayed G, Al-Sawahli MM. Hydrogel containing PEG-coated fluconazole nanoparticles with enhanced solubility and antifungal activity. *J Pharm Innov*. 2019;14(2):112-22. doi:10.1007/s12247-018-9335-z
- Longley N, Muzoora C, Taseera K, Mwesigye J, Rwebembera J, Chakera A, et al. Dose response effect of high-dose fluconazole for hiv-associated cryptococcal meningitis in southwestern uganda. *Clin Infect Dis*. 2008;47(12):1556-61. doi:10.1086/593194
- Koltin Y, Hitchcock CA. The search for new triazole antifungal agents. *Curr Opin Chem Biol*. 1997;1(2):176-82. doi:10.1016/s1367-5931(97)80007-5
- Nakarani M, Misra A, Patel J, Vaghani S. Itraconazole nanosuspension for oral delivery: Formulation, characterization and in vitro comparison with marketed formulation. *Daru*. 2010;18(2):84.
- Dash AK, Elmquist WF. Fluconazole. In: Brittain HG, editor. *Analytical profiles of drug substances and excipients*: Cambridge, Massachusetts: Academic Press; 2001. p. 67-113.
- Kastelic J, Kikelj D, Leban I, Lah N. Fluconazole-malonic acid (1/1). *Acta Crystallogr Sect E Struct Rep Online*. 2013;69(Pt 3):o378-o9. doi:10.1107/S1600536813003656
- Garipov MR, Pavelyev RS, Lisovskaya SA, Nikitina EV, Kayumov AR, Sabirova AE, et al. Fluconazole-pyridoxine bis-triazolium compounds with potent activity against pathogenic bacteria and fungi including their biofilm-embedded forms. *J Chem*. 2017;2017:4761650. doi:10.1155/2017/4761650
- Maeda T, Takenaka H, Yamahira Y, Noguchi T. Use of rabbits for gi drug absorption studies: Relationship between dissolution rate and bioavailability of griseofulvin tablets. *J Pharm Sci* 1979;68(10):1286-9. doi:10.1002/jps.2600681023
- Chiba Y, Kohri N, Iseki K, Miyazaki K. Improvement of dissolution and bioavailability for mebendazole, an agent for human echinococcosis, by preparing solid dispersion with polyethylene glycol. *Chem Pharm Bull (Tokyo)*. 1991;39(8):2158-60. doi:10.1248/cpb.39.2158
- El-Feky GS, Zayed G, Farrag ARH. Optimization of an ocular nanosuspension formulation for acyclovir using factorial design. *Int J Pharm Pharm Sci*. 2013;5(SUPPL 1):213-9.
- Merisko-Liversidge E, Sarpotdar P, Bruno J, Hajj S, Wei L, Peltier N, et al. Formulation and antitumor activity evaluation of nanocrystalline suspensions of poorly soluble anticancer drugs. *Pharm Res*. 1996;13(2):272-8. doi:10.1023/a:1016051316815
- Müller RH, Peters K. Nanosuspensions for the formulation of poorly soluble drugs: I. Preparation by a size-reduction technique. *Int J Pharm*. 1998;160(2):229-37. doi:10.1016/S0378-5173(97)00311-6
- Siekmann B, Westesen K. Preparation and physicochemical characterization of aqueous dispersions of coenzyme q 10 nanoparticles. *Pharm Res*. 1995;12(2):201-8. doi:10.1023/A:1016270724413
- Müller RH. *Colloidal carriers for controlled drug delivery and targeting: Modification, characterization and in vivo distribution*. Oxfordshire: Taylor & Francis; 1991.
- Moazeni M, Kelidari HR, Saeedi M, Morteza-Semnani K, Nabili M, Gohar AA, et al. Time to overcome fluconazole resistant candida isolates: Solid lipid

- nanoparticles as a novel antifungal drug delivery system. *Colloids Surf B*. 2016;142:400-7. doi:10.1016/j.colsurfb.2016.03.013
20. Kelidari HR, Moazeni M, Babaei R, Saeedi M, Akbari J, Parkoohi PI, et al. Improved yeast delivery of fluconazole with a nanostructured lipid carrier system. *Biomed Pharmacother*. 2017;89:83-8. doi:10.1016/j.biopha.2017.02.008
21. Moazeni M, Saeedi M, Kelidari H, Nabili M, Davari A. An update on the application of nano-scaled carriers against fluconazole-resistant candida species: Nanostructured lipid carriers or solid lipid nanoparticles? *Curr Med Mycol*. 2019;5(4):8. doi:10.18502/CMM.5.4.1965
22. Putra OD, Umeda D, Nugraha YP, Furuishi T, Nagase H, Fukuzawa K, et al. Solubility improvement of epalrestat by layered structure formation via cocrystallization. *CrystEngComm*. 2017;19(19):2614-22. doi:10.1039/C7CE00284J
23. Akbari J, Saeedi M, Enayatifard R, Morteza-Semnani K, Hashemi SMH, Babaei A, et al. Curcumin niosomes (curcusesomes) as an alternative to conventional vehicles: A potential for efficient dermal delivery. *J Drug Deliv Sci Technol*. 2020;60:102035. doi:10.1016/j.jddst.2020.102035
24. Enayatifard R, Akbari J, Saeedi M, Morteza-Semnani K, Parvin S, Hashemi MH, et al. Investigating the effect of coated lipid nano particles of spirinolactone with chitosan on their properties. *J Mazandaran Univ Med Sci*. 2018;28(162):25-36.
25. Tajbakhsh M, Saeedi M, Akbari J, Morteza-Semnani K, Nokhodchi A, Hedayatizadeh-Omran A. An investigation on parameters affecting the optimization of testosterone enanthate loaded solid nanoparticles for enhanced transdermal delivery. *Colloids Surf A Physicochem Eng Asp*. 2020;589:124437. doi:10.1016/j.colsurfa.2020.124437
26. Zayed GM, Kamal I, Abdelhafez WA, M. Alsharif F, Amin MA, Shaykoon MSA, et al. Effect of chemical binding of doxorubicin hydrochloride to gold nanoparticles, versus electrostatic adsorption, on the in vitro drug release and cytotoxicity to breast cancer cells. *Pharm Res*. 2018;35(6):112. doi:10.1007/s11095-018-2393-6
27. Guo D, Dou D, Li X, Zhang Q, Bhutto ZA, Wang L. Ivermectin-loaded solid lipid nanoparticles: Preparation, characterisation, stability and transdermal behaviour. *Artif Cells Nanomed Biotechnol*. 2018;46(2):255-62. doi:10.1080/21691401.2017.1307207
28. Khezri K, Saeedi M, Morteza-Semnani K, Akbari J, Rostamkalaei SS. An emerging technology in lipid research for targeting hydrophilic drugs to the skin in the treatment of hyperpigmentation disorders: Kojic acid-solid lipid nanoparticles. *Artif Cells Nanomed Biotechnol*. 2020;48(1):841-53. doi:10.1080/21691401.2020.1770271
29. Wayne P. Clinical and laboratory standards institute (clsi): Reference method for broth dilution antifungal susceptibility testing of filamentous fungi. Allured Publishing Corporation: Carol Stream, IL, USA; 2008. https://clsi.org/media/1455/m38a2_sample.pdf
30. Enayatifard R, Akbari J, Babaei A, Rostamkalaei SS, Hashemi SMh, Habibi E. Anti-microbial potential of nano-emulsion form of essential oil obtained from aerial parts of *origanum vulgare* l. As food additive. *Adv Pharm Bull*. 2021;11(2):327-34. doi:10.34172/apb.2021.028
31. Rostamkalaei SS, Akbari J, Saeedi M, Morteza-Semnani K, Nokhodchi A. Topical gel of metformin solid lipid nanoparticles: A hopeful promise as a dermal delivery system. *Colloids Surf B*. 2019;175:150-7. doi:10.1016/j.colsurfb.2018.11.072
32. Xia D, Quan P, Piao H, Piao H, Sun S, Yin Y, et al. Preparation of stable nitrendipine nanosuspensions using the precipitation-ultrasonication method for enhancement of dissolution and oral bioavailability. *Eur J Pharm Sci*. 2010;40(4):325-34. doi:10.1016/j.ejps.2010.04.006
33. Housaindokht MR, Pour AN. Study the effect of hlb of surfactant on particle size distribution of hematite nanoparticles prepared via the reverse microemulsion. *Solid State Sci*. 2012;14(5):622-5. doi:10.1016/j.solidstatesciences.2012.01.016
34. Dillen K, Vandervoort J, Van den Mooter G, Ludwig A. Evaluation of ciprofloxacin-loaded eudragit® rs100 or rl100/plga nanoparticles. *Int J Pharm*. 2006;314(1):72-82. doi:10.1016/j.ijpharm.2006.01.041
35. Murakami H, Kobayashi M, Takeuchi H, Kawashima Y. Preparation of poly (dl-lactide-co-glycolide) nanoparticles by modified spontaneous emulsification solvent diffusion method. *Int J Pharm*. 1999;187(2):143-52. doi:10.1016/s0378-5173(99)00187-8
36. Matlhola K, Katata-Seru L, Tshweu L, Bahadur I, Makgatho G, Balogun M. Formulation and optimization of eudragit rs po-tenofovir nanocarriers using box-behnken experimental design. *J Nanomater*. 2015;2015:630690. doi:10.1155/2015/630690
37. Shid RL, Dhole SN, Kulkarni N, Shid SL. Formulation and evaluation of nanosuspension delivery system for simvastatin. *Int J Pharm Sci Nanotechnol*. 2014;7:2459-76. doi:10.37285/ijpsn.2014.7.2.8
38. Morschhäuser J. Regulation of multidrug resistance in pathogenic fungi. *Fungal Genet Biol*. 2010;47(2):94-106. doi:10.1016/j.fgb.2009.08.002
39. Mishra N, Prasad T, Sharma N, Payasi A, Prasad R, Gupta D, et al. Pathogenicity and drug resistance in *candida albicans* and other yeast species. *Acta Microbiol Immunol Hung*. 2007;54(3):201-35. doi:10.1556/AMicr.54.2007.3.1
40. Bianchin MD, Borowicz SM, Machado GdRM, Pippi B, Guterres SS, Pohlmann AR, et al. Lipid core nanoparticles as a broad strategy to reverse fluconazole resistance in multiple candida species. *Colloids Surf B*.

- 2019;175:523-9. doi:10.1016/j.colsurfb.2018.12.011
41. Mathieu V, Pirker C, Martin de Lassalle E, Vernier M, Mijatovic T, DeNeve N, et al. The sodium pump alpha1 sub-unit: A disease progression-related target for metastatic melanoma treatment. *J Cell Mol Med.* 2009;13(9B):3960-72. doi:10.1111/j.1582-4934.2009.00708.x
42. Somchit N, Hassim SM, Samsudin SH. Itraconazole and fluconazole-induced toxicity in rat hepatocytes: A comparative in vitro study. *Hum Exp Toxicol.* 2002;21(1):43-8. doi:10.1191/0960327102ht208oa
43. Correa RM, Mota TC, Guimarães AC, Bonfim LT, Burbano RR, Bahia MD. Cytotoxic and genotoxic effects of fluconazole on african green monkey kidney (vero) cell line. *BioMed Res Int.* 2018;2018:6271547. doi:10.1155/2018/6271547